Evolutionary pathways to antibiotic resistance are dependent upon environmental structure and bacterial lifestyle

Alfonso Santos-Lopez*[1], Christopher W. Marshall*[1], Michelle R. Scribner[1], Daniel Snyder[1,2] and Vaughn S. Cooper[1,2,3]

[1]*Department of Microbiology and Molecular Genetics, and Center for Evolutionary Biology and Medicine, University of Pittsburgh, Pittsburgh, Pennsylvania, USA.*

[2]*Microbial Genome Sequencing Center, University of Pittsburgh, Pittsburgh, Pennsylvania, USA.*

[3]*Center for Evolutionary Biology and Medicine, University of Pittsburgh, Pittsburgh, Pennsylvania, USA.*

*A.S-L. and C.W.M. contributed equally to this manuscript

Abstract

Bacterial populations vary in their stress tolerance and population structure depending upon whether growth occurs in well-mixed or structured environments. We hypothesized that evolution in biofilms would generate greater genetic diversity than well-mixed environments and lead to different pathways of antibiotic resistance. We used experimental evolution and whole genome sequencing to test how the biofilm lifestyle influenced the rate, genetic mechanisms, and pleiotropic effects of resistance to ciprofloxacin in *Acinetobacter baumannii* populations. Both evolutionary dynamics and the identities of mutations differed between lifestyle. Planktonic populations experienced selective sweeps of mutations including the primary topoisomerase drug targets, whereas biofilm-adapted populations acquired mutations in regulators of efflux pumps. An overall trade-off between fitness and resistance level emerged, wherein biofilm-adapted clones were less resistant than planktonic but more fit in the absence of drug. However, biofilm populations developed collateral sensitivity to cephalosporins, demonstrating the clinical relevance of lifestyle on the evolution of resistance.

30 **Introduction**

31 Antimicrobial resistance (AMR) is one of the main challenges facing modern medicine.
32 The emergence and rapid dissemination of resistant bacteria is decreasing the
33 effectiveness of antibiotics and it is estimated that 700,000 people die per year due to
34 AMR-related problems (O´Neill, 2016). AMR, like all phenotypes, is an evolved
35 property, either the ancient product of living amidst other microbial producers of
36 antimicrobials (Martínez, 2008), or the recent product of strong selection by human
37 activities for novel resistance-generating mutations (Ventola, 2015).

38

39 The dominant mode of growth for most microbes is on surfaces, and this biofilm lifestyle
40 is central to AMR (Ahmed, Porse, Sommer, Hoiby, & Ciofu, 2018; Hoiby, Bjarnsholt,
41 Givskov, Molin, & Ciofu, 2010; Olsen, 2015), especially in chronic infections (Wolcott,
42 2017; Wolcott et al., 2010). However, with few exceptions (Ahmed et al., 2018; France,
43 Cornea, Kehlet-Delgado, & Forney, 2019; Ridenhour et al., 2017), most of the research
44 on the evolution of AMR has been conducted in well-mixed populations [reviewed in
45 (Hughes & Andersson, 2017)] or on agar plates (Michael Baym et al., 2016), conditions
46 that cannot simulate the effects of biofilms on the evolution of AMR. Consequently, our
47 understanding of how this lifestyle influences the evolution of AMR, whether by different
48 population-genetic dynamics or molecular mechanisms, is limited. One example is that
49 the close proximity of cells in biofilms may facilitate the horizontal transfer and
50 persistence of resistance genes in bacterial populations (Ridenhour et al., 2017; Stalder &
51 Top, 2016). Less appreciated is the potential for the biofilm lifestyle to influence the
52 evolution of AMR by *de novo* chromosomal mutations. This emergence of AMR in
53 biofilms is important because: i) the environmental structure of biofilms can increase
54 clonal interference, rendering selection less effective and enhancing genetic diversity

55 (Cooper, Staples, Traverse, & Ellis, 2014; Ellis, Traverse, Mayo-Smith, Buskirk, &
56 Cooper, 2015; France et al., 2019; Habets, Rozen, Hoekstra, & de Visser, 2006; Traverse,
57 Mayo-Smith, Poltak, & Cooper, 2013), ii) distinct ecological conditions within the
58 biofilm can favor functionally distinct adaptations to different niches (Poltak & Cooper,
59 2011), iii) the biofilm itself can protect its residents from being exposed to external
60 stresses like antibiotics or host immunity (Eze, Chenia, & El Zowalaty, 2018; E. Geisinger
61 & Isberg, 2015), and iv) slower growth within biofilms can reduce the efficacy of
62 antibiotics that preferentially attack fast-growing cells (Kirby, Garner, & Levin, 2012;
63 Walters, Roe, Bugnicourt, Franklin, & Stewart, 2003). The first two hypotheses would
64 predict more complex evolutionary dynamics within biofilms than in well-mixed
65 environments (Steenackers, Parijs, Foster, & Vanderleyden, 2016), while the second two
66 predict different rates of evolution, targets of selection, and likely less potent mechanisms
67 of AMR (Andersson & Hughes, 2014). Together, these potential factors call into question
68 the conventional wisdom of a tradeoff between fitness and antimicrobial resistance, a
69 relationship that remains to be clearly defined.
70
71 Here, we study the evolutionary dynamics and effects of new resistance mutations in the
72 opportunistic nosocomial pathogen *Acinetobacter baumannii*, which is often intrinsically
73 resistant to antibiotics or has been reported to rapidly evolve resistance to them (Doi,
74 Murray, & Peleg, 2015). This pathogen is categorized as one of the highest threats to
75 patient safety (Asif, Alvi, & Rehman, 2018), partly due to its ability to live on inanimate
76 surfaces in biofilms (Eze et al., 2018). We experimentally propagated populations of *A.*
77 *baumannii* exposed either to subinhibitory or increasing concentrations of ciprofloxacin
78 (CIP) over 80 generations in biofilm or planktonic conditions to ascertain whether these
79 lifestyles select for different mechanisms of AMR. Rather than focusing on the genotypes

80 of single isolates, which can limit the scope of an analysis, we conducted whole-
81 population genomic sequencing over time to define the dynamics of adaptation and the
82 fitness of certain resistance alleles compared to others in the experiment. We then
83 identified clones with specific genotypes that we linked to fitness and resistance
84 phenotypes. This approach sheds new light on the ways that pathogens adapt to antibiotics
85 while growing in biofilms and has implications for treatment decisions.
86

87 **Results and Discussion**

88 **1. Experimental evolution**

89 Replicate cultures of the susceptible *A. baumannii* strain ATCC 17978 (Baumann,
90 Doudoroff, & Stanier, 1968; Piechaud & Second, 1951) were established under
91 planktonic or biofilm conditions in one of three treatments: i) no antibiotics, ii) sub-
92 inhibitory concentration of the antibiotic ciprofloxacin (CIP) and iii) evolutionary rescue
93 (Bell & Gonzalez, 2009) in which CIP concentrations were increased every 72 hours from
94 subinhibitory concentrations to four times the minimum inhibitory concentration (MIC)
95 (Figure 1A). Before the start of the antibiotic evolution experiment, we propagated the
96 ATCC strain for ten days in planktonic conditions to reduce the influence of adaptation
97 to the laboratory conditions on subsequent comparisons. CIP was chosen because of its
98 clinical importance in treating *A. baumannii* (Ardebili, Lari, & Talebi, 2014; Doi et al.,
99 2015; Lopes & Amyes, 2013), its ability to penetrate the biofilm matrix (Tseng et al.,
100 2013) allowing similar efficacy in well mixed and structured populations (Kirby et al.,
101 2012), and because it is not known to stimulate biofilm formation in *A. baumannii* (Aka
102 & Haji, 2015). Planktonic populations were serially passaged by daily 1:100 dilution
103 while biofilm populations were propagated using a bead model simulating the biofilm life
104 cycle (Poltak & Cooper, 2011; Traverse et al., 2013; Turner, Marshall, & Cooper, 2018).

105 This model selects for bacteria that attach to a 7 mm polystyrene bead, form a biofilm,
106 and then disperse to colonize a new bead each day. (A video tutorial for this protocol is
107 available at http://evolvingstem.org). The transfer population size in biofilm and in
108 planktonic cultures was set to be nearly equivalent at the beginning of the experiment
109 (approximately $1x10^7$ CFU/mL), because population size influences mutation availability
110 and the response to selection (Cooper, 2018; Salverda, Koomen, Koopmanschap, Zwart,
111 & de Visser, 2017). The mutational dynamics of three lineages from each treatment were
112 tracked by whole-population genomic sequencing (Figure 1A). We also sequenced 49
113 single clones isolated from 22 populations at the end of the 12-day experiment to
114 determine mutation linkage.
115
116 **2. Evolution of CIP resistance**
117 The rate and extent of evolved resistance depends on the strength of antibiotic selection
118 (Andersson & Hughes, 2014; Oz et al., 2014), the distribution of fitness effects of
119 mutations that increase resistance to the drug (Maclean, Hall, Perron, & Buckling, 2010),
120 and the population size of replicating bacteria (Cooper, 2018; Salverda et al., 2017). The
121 mode of bacterial growth can in principle alter each of these three variables and generate
122 different dynamics and magnitudes of AMR. In the populations exposed to the increasing
123 concentrations of CIP (the evolutionary rescue), the magnitude of evolved CIP resistance
124 differed between planktonic and biofilm populations. Planktonic populations became
125 approximately 160x more resistant on average than the ancestral clone while the biofilm
126 populations became only 6x more resistant (Figure 1B and Table S1). Planktonic
127 populations also evolved resistance much more rapidly, becoming 10x more resistant
128 after only 24 hours of growth in sub-inhibitory CIP. This level of resistance would have
129 been sufficient for surviving the remainder of the experiment, but MICs continued to

130 increase at each sampling (Figure 1B). The evolution of resistance far beyond the
131 selective requirement indicates that mutations conferring higher resistance also increased
132 fitness in planktonic populations exposed to CIP.
133
134 In contrast, biofilm-evolved populations evolved under the evolutionary rescue regime
135 acquired much lower levels of resistance (*ca.* 3– 7x the ancestral MIC) and primarily in
136 a single step between days 3 and 4 (Figure 1B). In one notable exception, the MIC of
137 biofilm population B2 increased ~50x after 3 days of selection in subinhibitory
138 concentrations of CIP (Figure 1B), but then the resistance of this population declined to
139 only 6x higher than the ancestral strain. This dynamic suggested that a mutant conferring
140 high-level resistance rose to intermediate frequency but was replaced by a more fit, yet
141 less resistant, mutant (this possibility is evaluated below).
142
143 Lower levels of resistance were observed in populations selected at constant subinhibitory
144 concentrations of CIP. Biofilm populations were 4x more resistant than the ancestor and
145 planktonic populations were 20x more resistant (Table S1). We can infer that biofilm
146 growth does not select for the high-level resistance seen in planktonic populations, instead
147 favoring mutants with low levels of resistance and better adapted to life in a biofilm. It is
148 important to note that these MIC measurements were made in planktonic conditions
149 according to the clinical standards (CLSI, 2007) and that these values increased when
150 measured in biofilm (Table S2). Our results correspond with studies of clinical isolates in
151 which those producing more biofilm (and likely having adapted in biofilm conditions)
152 were less resistant than non-biofilm-forming isolates (Wang et al., 2018). Nevertheless,
153 measuring growth and MIC is context-dependent (Borriello et al., 2004; Hill et al., 2005;
154 Kirby et al., 2012), and because the biofilm environment at least partially protects cells

155 from antibiotic exposure (Table S2), it can be argued that evolved biofilm populations
156 experienced lower CIP concentrations than planktonic populations. However, we selected
157 CIP because it can penetrate the biofilm barrier (Tseng et al., 2013), and furthermore,
158 cells growing in the bead model must disperse from one bead to colonize the next one in
159 a less protected state. Overall, these results demonstrate that exposing bacteria to low
160 levels of antibiotic risks selection for high levels of resistance that can make future
161 treatment more difficult (Wistrand-Yuen et al., 2018).
162
163 **3. Evolutionary dynamics under CIP treatment**
164 In large bacterial populations (>10^5 cells) growing under strong selection, adaptive
165 mutations conferring beneficial traits such as antibiotic resistance will dominate
166 population dynamics (Jeffrey E Barrick & Lenski, 2013; Cooper, 2018). Therefore, if a
167 single mutation renders the antibiotic ineffective and provides the highest fitness gain, it
168 would be expected to outcompete all other less fit mutations. Further, the stronger the
169 selection for resistance, the greater the probability of genetic parallelism among replicate
170 populations (Bolnick, Barrett, Oke, Rennison, & Stuart, 2018). Under the conditions of
171 these experiments, approximately 10^6 mutations occur in the first growth cycle and
172 roughly 10^7 mutations arise over the 12 days of selection, leading to a probability of 0.98
173 that every site in the 4Mbp *A. baumannii* genome experiences a mutation at least once
174 over the course of the 12-day experiment (see Table S3 for details of these calculations).
175 The dramatic differences in the evolved resistance levels of planktonic and biofilm
176 populations suggested distinct genetic causes of resistance resulting from different
177 selective forces in these treatments. We also predicted greater genetic diversity in the
178 biofilm treatments, owing to spatial structure and/or niche differentiation (Traverse et al.,
179 2013), than in the planktonic cultures, in which we expected selective sweeps (Jeffrey E.

180 Barrick et al., 2009). A signature of spatial structure alone might be different mutations
181 in the same gene with predicted similar function coexisting over time, which is a form of
182 clonal interference (de Visser & Rozen, 2006). A signature of niche differentiation might
183 be the coexistence of mutations in different genes with unique functions, which is a form
184 of adaptive radiation (Kassen, 2009).
185
186 We conducted whole-population genomic sequencing of three replicates per treatment to
187 identify all contending mutations above a detection threshold of 5% (see Methods). The
188 spectrum of mutations from CIP-treated populations are consistent with expectations
189 from strong positive selection on altered or disrupted coding sequences (see Table 1 for
190 day-12 results and Table S4 for dynamics across the experiment). High nonsynonymous
191 to synonymous mutation ratios were observed in both lifestyles (8.5 in planktonic and 9.7
192 in biofilm). 43% of the total mutations in planktonic and 34% in biofilm were insertions
193 or deletions, which is vastly enriched over typical mutation rates of ~10 SNPs/indel under
194 neutral conditions (Dillon, Sung, Sebra, Lynch, & Cooper, 2017; Lynch et al., 2016).
195 Roughly 30% of the mutations in CIP-treated populations of either lifestyle occurred in
196 intergenic regions (30% in planktonic-propagated populations and 32% in biofilm). Of
197 the intergenic mutations, 72% of the planktonic mutations and 18% of the biofilm
198 mutations occurred in promoters, 5' untranslated regions, or in putative terminators
199 (Kröger et al., 2018).
200
201 As expected from theory, in CIP-selected planktonic populations where selection is most
202 efficient, one or two mutations rapidly outcompeted others and fixed (Figure 2). Selection
203 in biofilms, however, produced fewer selective sweeps and maintained more contending
204 mutations, especially at lower antibiotic concentrations. In one population, multiple

205 mutations in the same locus (*adeL*) rose to high frequency and persisted, which is
206 consistent with the effect of population structure alone. In the other two populations,
207 mutations in different efflux pumps (*adeL, adeS, adeN*) contended during the experiment,
208 which could be explained by population structure or ecological diversification, if these
209 mutations produced different phenotypes. Overall, across all treatments and timepoints,
210 biofilm-adapted populations were significantly more diverse than the planktonic-adapted
211 populations (Shannon index; Kruskal Wallis, chi-squared = 7.723, p = 0.005), particularly
212 at subinhibitory concentrations of CIP (Figure S1A). Notably, increasing drug
213 concentrations eliminated the differences in diversity between treatments (Figure S1B),
214 but the greater diversity in biofilms treated with lower doses generated more diversity for
215 selection to act upon in a changing environment. This higher standing diversity is
216 important when considering dosing and when antibiotic exposure may be low (*e.g.* in the
217 external environment or when bound to tissues) (Baquero, Negri, Morosini, & Blazquez,
218 1998; Khan, Berglund, Khan, Lindgren, & Fick, 2013) because biofilms with more allelic
219 diversity have a greater chance of survival to drug and immune attack (Fux, Costerton,
220 Stewart, & Stoodley, 2005).
221
222 In contrast with the data observed in the populations evolving under CIP pressure, drug-
223 free control populations contained no mutations that achieved high frequency during the
224 experiment (Figures 2C and 2D). These results suggest that the ancestral starting clone
225 was already well-adapted to our experimental conditions, likely because we had
226 previously propagated the *A. baumannii* ATCC 17978 clone under identical drug-free
227 conditions for 10 days. This preadaptation phase led to the fixation of mutations in three
228 genes (Table S5).
229

230 **4. Lifestyle determines the selected mechanisms of resistance**

231 *A. baumannii* clinical samples acquire resistance to CIP by two principal mechanisms:
232 modification of the direct antibiotic targets — gyrase A or B and topoisomerase IV — or
233 by the overexpression of efflux pumps reducing the intracellular concentrations of the
234 antibiotic (Doi et al., 2015). To directly associate genotypes with resistance phenotypes,
235 we sequenced 49 clones isolated at the end of the experiment, the majority of which were
236 selected to delineate genotypes in the evolutionary rescue populations (Figures 2F and
237 S2).

238

239 Both the genetic targets and mutational dynamics of selection in planktonic and biofilm
240 environments differed. Mutations disrupting three negative regulators of efflux pumps
241 evolved in parallel across populations exposed to CIP, but mutations in two of these (*adeL*
242 and *adeS*) were nearly exclusive to biofilm clones (Figure 2F). The most common and
243 highest frequency mutations observed in the biofilm populations were in the repressor
244 gene *adeL* (Figures 2F, S2, and Table S6), which regulates AdeFGH, one of three
245 resistance-nodulation-division (RND) efflux pump systems in *A. baumannii* (Coyne,
246 Rosenfeld, Lambert, Courvalin, & Perichon, 2010; Fernando, Zhanel, & Kumar, 2013;
247 Pournaras, Koumaki, Gennimata, Kouskouni, & Tsakris, 2016). In the planktonic lines,
248 the predominant mutations were found in *adeN,* which is a negative regulator of AdeIJK
249 and were mainly insertions of IS701 that disrupted the gene (X.-Z. Li, C. A. Elkins, & H.
250 I. Zgurskaya, 2016).

251

252 In biofilm lines, different contending *adeL* mutations were detected in each replicate after
253 24 hours then eventually fixed as CIP concentrations increased (green lines in Figure 2B),
254 sometimes along with a secondary *adeL* mutation. This pattern suggests that altering

255 efflux via *adeL* generates adaptations to the combination of CIP and biofilm which is
256 supported by the increase in biofilm formation by the *adeL* mutants (Figure S3). Further,
257 mutants with higher resistance than necessary appear to be maladaptive in the biofilm
258 treatment. For example, *adeN* (found more often in planktonic culture) and *adeS*
259 mutations found simultaneously on day 3 in population B2 (Figure 2) led to a spike in
260 resistance at that timepoint (Figure 1), but these alleles were subsequently outcompeted
261 by *adeL* mutants that were evidently more fit despite lower planktonic resistance.
262
263 In contrast to the biofilm populations, all planktonic populations with increasing
264 concentrations of CIP eventually acquired a single high frequency mutation in *gyrA*
265 (S81L), the canonical ciprofloxacin-resistant mutation in DNA gyrase. These *gyrA*
266 mutations evolved in genetic backgrounds containing either an *adeN* mutant or a *pgpB*
267 mutant. *pgpB* is a gene that encodes a putative membrane associated lipid phosphatase
268 and is co-regulated by *adeN* (Hua, Chen, Li, & Yu, 2014). Other mutations associated
269 with high levels of resistance affected *parC,* encoding topoisomerase IV, and regulatory
270 regions of two putative transporters, ACX60_RS15145 and ACX60_RS1613, the latter
271 being co-transcribed with the multidrug efflux pump *abeM* (Su, Chen, Mizushima,
272 Kuroda, & Tsuchiya, 2005). Few other mutations exceeded the 10% of the total
273 population filter in the planktonic lines. The rapid fixation of only *adeN* and *adeN*-
274 regulated alleles in the planktonic CIP-exposed populations indicate that *adeN* conferred
275 higher fitness than other CIP-resistant mutations at low drug concentrations.
276 Subsequently, at increased concentrations of CIP, on-target mutations in *gyrA* were
277 favored in each line.
278

279 Together, our results demonstrate that bacterial lifestyle influences the evolutionary
280 dynamics and targets of selection of AMR. Loss-of-function mutations in regulators of
281 the *adeFGH* and *adeABC* RND efflux pumps that increased CIP resistance ~4-fold in
282 biofilm populations treated with CIP. Adaptation by planktonic populations exposed to
283 CIP proceeded first by altering the *adeN*-controlled *adeIJK* efflux pump and then by
284 directly altering the targets of the fluoroquinolone, *gyrA* and *parC*, leading to much higher
285 levels of resistance.
286
287 **5. Evolutionary consequences of acquiring resistance**
288 The large population sizes (10^7 – 10^9 cells) and number of generations (~80) in all evolved
289 lines mean that similar mutations very likely arose in each replicate regardless of
290 treatment, meaning that the success of some mutations over others reflects their greater
291 fitness in that condition (Table S3) (Cooper, 2018). Yet *de novo* acquired antibiotic
292 resistance is often associated with a fitness cost in the absence of antibiotics [reviewed in
293 (Vogwill & MacLean, 2015)]. The extent of this cost and the ability to compensate for it
294 by secondary mutations (compensatory evolution) is a key attribute determining the
295 spread and maintenance of the resistance mechanism (Maclean et al., 2010; Moore,
296 Rozen, & Lenski, 2000; Vogwill & MacLean, 2015; Zhao & Drlica, 2002). A negative
297 correlation between CIP resistance and fitness of resistant genotypes in the absence of
298 antibiotics has been previously described in *Escherichia coli,* suggesting a trade-off
299 between these traits (Basra et al., 2018; Huseby et al., 2017; Marcusson, Frimodt-Moller,
300 & Hughes, 2009).
301
302 To determine the relationship between resistance and fitness in the absence of antibiotics
303 in our experiment, we chose 10 clones (5 each from biofilm and planktonic populations,

304 Figures 2F and S2) with different genotypes and putative resistance mechanisms and
305 measured their resistance and fitness phenotypes in both planktonic and biofilm
306 conditions (Figure 3). As expected from the populations (Figure 1B), the biofilm clones
307 much were less resistant in planktonic conditions than those evolved planktonically [MIC
308 = 0.58 mg/L (SEM = 0.13) vs. MIC = 8.53 mg/L (SEM = 1.96), two-tailed t-test: $p < 0.05$,
309 $t = 4.048$, df = 80]. However, biofilm-evolved clones were more fit relative to the
310 ancestral strain than the planktonic-evolved clones in the absence of antibiotic (two-tailed
311 t-test: $p = 0.008$, $t = 2.984$ df = 18) (Figure 3). Importantly, these fitness measurements
312 were made in both planktonic and biofilm conditions, demonstrating that even in the
313 conditions they evolved in, the planktonic selected clones were less fit as a result of
314 antibiotic resistance trade-offs. However, one planktonic-evolved clone with mutations
315 in both *gyrA* and *parC* exhibited no significant fitness cost and high levels of resistance.
316 This suggests that, as in *Pseudomonas aeruginosa*, the *parC* mutation may compensate
317 for the cost imposed by *gyrA* mutation (Kugelberg, Lofmark, Wretlind, & Andersson,
318 2005), an example of sign epistasis (Sackman & Rokyta, 2018). Overall, mutants selected
319 in biofilm-evolved populations were less resistant than mutants selected in planktonic
320 populations (Figure 1B) but produced more biofilm (Figure S3) and paid little or no
321 fitness cost in the absence of antibiotics (Figures 3). This cost-free resistance implies that
322 these subpopulations could persist in the absence of drug, limiting the treatment options
323 and demanding new approaches to treat high fitness, resistant pathogens (Baym, Stone,
324 & Kishony, 2016).
325
326 **6. Evolutionary interactions with other antibiotics**
327 When a bacterium acquires resistance to one antibiotic, the mechanism of resistance can
328 also confer resistance to other antibiotics (cross-resistance) or increase the susceptibility

329 to other antibiotics (collateral sensitivity) (Pal, Papp, & Lazar, 2015). We tested the MIC
330 of the evolved populations to 23 different antibiotics in planktonic conditions. We
331 observed changes in susceptibilities to 13 of the 23 antibiotics tested, and these changes
332 were growth mode dependent (Figure 4). For example, planktonic populations exhibited
333 cross resistance to cefpodoxime and ceftazidime, but biofilm populations evolved
334 collateral sensitivity to these cephalosporins. Cross-resistance was associated genetically
335 with *adeN, adeS, gyrA* or *pgpB* mutations, and collateral sensitivity was associated with
336 *adeL* mutations. Selection in these environments evidently favors the activation of
337 different efflux pumps or modified targets that have different pleiotropic consequences
338 for multidrug resistance (Podnecky et al., 2018).
339
340 The mechanisms leading to collateral sensitivity are still poorly understood but they
341 depend on the genetic background of the strain, the nature of the resistance mechanisms
342 (Barbosa et al., 2017; Yen & Papin, 2017), and the specific physiological context of the
343 cells (Leus et al., 2018). In *A. baumannii*, each RND efflux pump is suggested to be
344 specific for certain classes of antibiotics (Coyne, Courvalin, & Perichon, 2011; Leus et
345 al., 2018; X. Z. Li, C. A. Elkins, & H. I. Zgurskaya, 2016). Similar to our results (Figure
346 4), Yoon and collaborators demonstrated that efflux pumps AdeABC and AdeIJK,
347 regulated by *adeS* and *adeN* respectively, increased the resistance level to some β-lactams
348 when overexpressed (Yoon et al., 2015). However, production of AdeFGH, the efflux
349 pump regulated by *adeL,* decreased resistance to some β-lactams and other families of
350 antibiotics or detergents by an unknown mechanism (Leus et al., 2018; Yoon et al., 2015).
351 Increased sensitivity to β-lactams with efflux overexpression has also been reported in *P.*
352 *aeruginosa* (Azimi & Rastegar Lari, 2017), which demonstrates the urgency of
353 understanding the physiological basis of collateral sensitivity to control AMR evolution.

354 Exploiting collateral sensitivity has been proposed to counteract the evolution of resistant
355 populations both in bacteria (Imamovic & Sommer, 2013; Kim, Lieberman, & Kishony,
356 2014; Nichol et al., 2019) and in cancer (Dhawan et al., 2017). Remarkably, our results
357 show that biofilm growth, commonly thought to broaden resistance, may actually
358 generate collateral sensitivity during treatment with CIP and potentially other
359 fluoroquinolones.
360
361 **7. Clinical relevance**
362 Our results demonstrate that the mode of growth determines both the mechanism of
363 evolved resistance and the spectrum of sensitivity to other families of antibiotics. Further,
364 the mutations selected in our experimental conditions also play an important role in
365 clinical isolates, as fluoroquinolone resistance mediated by plasmids in *A. baumannii*
366 appears to be rare (Yang, Hu, Liu, Ye, & Li, 2016). The mutations S81L in *gyrA* and
367 S80L *in parC* acquired by the sensitive ATCC 17978 strain used in this study have been
368 reported worldwide as the primary mechanism conferring high levels of resistance to
369 fluorquinolones in clinical isolates (Adams-Haduch et al., 2008; Dahdouh et al., 2017;
370 W. A. Warner et al., 2016).
371
372 In addition to the on-target mechanisms of resistance through gyrase or topoisomerase
373 mutations, *A. baumannii* isolates acquire comparatively moderate levels of
374 fluoroquinolone resistance by modifications in various RND efflux pumps. These RND
375 efflux pumps have overlapping yet differing substrate profiles and may act synergistically
376 in increasing the resistance level (Table S7) (Coyne et al., 2010; Damier-Piolle, Magnet,
377 Bremont, Lambert, & Courvalin, 2008; Fernando et al., 2013; Rosenfeld, Bouchier,
378 Courvalin, & Perichon, 2012). In our experiment, all biofilm and planktonic populations

379 and nearly all isolated clones acquired mutations in at least one of the three regulators of
380 the RND efflux pumps (*adeL, adeS, adeN*) or in a gene regulated by one of these
381 regulators (*pgpB*). Mutations in *adeL* upregulate the expression of the RND efflux pump
382 AdeFGH (Figure 2, Table S7) that is associated with a multidrug resistant phenotype in
383 clinical isolates (Coyne et al., 2010; Fernando et al., 2013; Leus et al., 2018; Pournaras et
384 al., 2016). AdeL-AdeFGH genes are often highly expressed in infection isolates, which
385 could reflect adaptation to the biofilm lifestyle (Coyne et al., 2010; Fernando et al., 2013).
386 Further, overexpression of *adeG* is predicted to enhance transport of acylated homoserine
387 lactones, including quorum-sensing autoinducers, which can increase both drug
388 resistance and biofilm formation (Alav, Sutton, & Rahman, 2018; He et al., 2015).
389 However, in clinical isolates, overexpression of the AdeFGH pump is less common than
390 the AdeIJK efflux pump that is regulated by *adeN* (Rosenfeld et al., 2012; Yoon et al.,
391 2015). AdeIJK contributes to resistance to biocides, hospital disinfectants, and to both
392 intrinsic and acquired antibiotic resistance in *A. baumannii* (Damier-Piolle et al., 2008;
393 Rosenfeld et al., 2012) and may decrease biofilm formation, which could explain its
394 prevalence in planktonic populations here (Yoon et al., 2015). Perhaps more concerning,
395 this study demonstrates that the overexpression of RND efflux pumps as a resistance
396 mechanism may produce little fitness cost in *A. baumannii*, as has previously been
397 demonstrated in both *P. aeruginosa* and *Neisseria gonorrhoeae* (Olivares Pacheco,
398 Alvarez-Ortega, Alcalde Rico, & Martínez, 2017; D. M. Warner, Folster, Shafer, & Jerse,
399 2007).
400
401 **Conclusions**
402 We used experimental evolution of the opportunistic pathogen *A. baumannii* in both well-
403 mixed and biofilm conditions to examine how lifestyle influences the dynamics, diversity,

404 identity of genetic mechanisms, and direct and pleiotropic effects of resistance to a
405 common antibiotic. Experimental evolution is a powerful method of screening naturally
406 arising genetic variation for mutants that are the best fit in a defined condition (Cooper,
407 2018; Elena & Lenski, 2003; Van den Bergh, Swings, Fauvart, & Michiels, 2018). When
408 population sizes are large and reproductive rates are rapid, as they were here, the
409 probability that all possible single-step mutations that can increase both resistance and
410 fitness occurred in each population is very likely. The few mutations selected here as well
411 as their repeated order with increasing CIP concentrations demonstrates that these are the
412 most fit mutations in this *A. baumannii* strain and set of environmental conditions. The
413 prevalence of some of these mutations in clinical samples suggests that they too may have
414 been exposed to selection in similar conditions. Likewise, the absence of other mutations
415 reported in shotgun mutant screens of resistance in *A. baumannii* (Edward Geisinger et
416 al., 2018) means that these mutants produced less resistance, lower fitness, or both.
417 Evolution experiments hold promise for ultimately forecasting mutations selected by
418 different antimicrobials and anticipating treatment outcomes, including the
419 diversification of the pathogen population and the likelihood of collateral sensitivity or
420 cross-resistance (Brockhurst et al., 2019). Furthermore, knowledge of the prevailing
421 lifestyle of the pathogen population may be critically important for treatment design.
422 Most infections are likely caused by surface-attached populations (Wolcott, 2017;
423 Wolcott et al., 2010), and some treatments include cycling antibiotics that promote
424 biofilm as a primary response. For example, tobramycin is used for treating *P. aeruginosa*
425 in cystic fibrosis patients (Hamed & Debonnett, 2017) and promotes biofilm formation
426 (Hoffman et al., 2005; Linares, Gustafsson, Baquero, & Martinez, 2006), wherein the
427 evolution of antibiotic resistance without a detectable fitness cost may arise during
428 treatment. But the more diverse biofilm-adapted lineages in our experiments revealed a

429 striking vulnerability to cephalosporins, which could provide a new strategy for
430 treatment. Broader still, conventional wisdom has long held that the relationship between
431 resistance and fitness is antagonistic, and that the efficacy of many antimicrobials is aided
432 by a severe fitness cost of resistance (M. Baym et al., 2016; Hughes & Andersson, 2017;
433 Vogwill & MacLean, 2015). This study demonstrates that the form of the relationship
434 between fitness and resistance can be altered by the mode of growth, whereby biofilms
435 can align resistance and fitness traits. Continued efforts to determine how the fitness
436 landscape of various resistance pathways depends on the environment and its structure,
437 including growth mode, could produce a valuable forecasting tool to stem the rising AMR
438 tide.
439

440 **Methods**

441 **Experimental evolution**

442 Before the start of the antibiotic evolution experiment, we propagated well mixed tubes
443 founded by one clone of the susceptible *A. baumannii* strain ATCC 17978-mff (Baumann
444 et al., 1968; Piechaud & Second, 1951) in a modified M9 medium (referred to as $M9^+$)
445 containing 0.1 mM $CaCl_2$, 1 mM $MgSO_4$, 42.2 mM Na_2HPO_4, 22 mM KH2PO_4, 21.7 mM
446 NaCl, 18.7 mM NH_4Cl and 11.1 mM glucose and supplemented with 20 mL/L MEM
447 essential amino acids (Gibco 11130051), 10 mL/L MEM nonessential amino acids (Gibco
448 11140050), and 1 mL each of trace mineral solutions A, B, and C (Corning 25021-3Cl).
449 This preadaptation phase was conducted in the absence of antibiotics for 10 days (*ca.* 66
450 generations) with a dilution factor of 100 per day.
451 After the ten days of preadaptation to $M9^+$ medium, we selected a single clone and
452 propagated for 24 hours in $M9^+$ in the absence of antibiotic. We then subcultured this
453 population into twenty replicate populations. Ten of the populations (5 planktonic and 5

454 biofilm) were propagated every 24 hours in constant subinhibitory concentrations of CIP,
455 0.0625 mg/L, which corresponds to 0.5x the minimum inhibitory concentration (MIC).
456 After 72 hours under subinhibitory concentrations of CIP, the populations were exposed
457 to two different antibiotic regimes for 9 more days, either constant subinhibitory
458 concentrations of CIP or increasing concentrations of CIP (called the evolutionary
459 rescue). For the latter, we doubled the CIP concentrations every 72 hours until 4x MIC.
460 As a control, the 20 remaining populations were propagated in the absence of CIP (Figure
461 1).
462
463 We propagated the populations into fresh media every 24 hours as described by Turner *et*
464 *al.* 2018 (Turner et al., 2018). For planktonic populations, we transferred a 1:100 (50 µl
465 into 5 mL of $M9^{+}$) dilution, which corresponded to 6.64 generations per day. For biofilm
466 populations, we transferred a polystyrene bead (Polysciences, Inc., Warrington, PA) to
467 fresh media containing three sterile beads. We rinsed each bead in PBS before the
468 transfer, therefore reducing the transfer of planktonic cells. Each day we alternated
469 between black and white marked beads, ensuring that the bacteria were growing on the
470 bead for 24 hours, which corresponds to approximately 6 to 7.5 generations/day (Traverse
471 et al., 2013; Turner et al., 2018). For the experiment with increasing concentrations of
472 antibiotics, we froze a sample of each bacterial population on days 1, 3, 4, 6, 7, 9, 10 and
473 12. In the experiment with constant exposure to subinhibitory concentrations of
474 antibiotics, we froze the populations on days 1, 3, 4, 9, and 12. We froze the control
475 populations at days 1, 4, 9, and 12. For planktonic populations, we froze 1 mL of culture
476 with 9% of DMSO. For freezing the biofilm populations, we sonicated the beads in 1 mL
477 of PBS with a probe sonicator and subsequently froze with 9% DMSO.
478

479 **Phenotypic characterization: antimicrobial susceptibility and biofilm formation**

480 We determined the MIC of CIP by broth microdilution in $M9^+$ according to the Clinical
481 and Laboratory Standards Institute guidelines (CLSI, 2007), in which each bacterial
482 sample was tested to 2-fold-increasing concentration of CIP from 0.0625 to 64 mg/L. To
483 obtain a general picture of the resistance profiles we determined the MIC to 23 antibiotics
484 (amikacin, ampicillin, ampicillin/sulbactam, aztreonam, cefazolin, cefepime,
485 cephalothin, meropenem, ertapenem, cefuroxime, gentamicin, CIP,
486 piperacillin/tazobactam, cefoxitin, trimethoprim/sulfamethoxazole, cefpodoxime,
487 ceftazidime, tobramycin, tigecycline, ticarcillin/clavulanic acid, ceftriaxone and
488 tetracycline) by broth microdilution in commercial microtiter plates following the
489 instructions provided by the manufacturers (Sensititre GN3F, Trek Diagnostics Inc.,
490 Westlake, OH). We tested the MIC at days 1, 3, 4, 6, 7, 9, 10 and 12 for the populations
491 propagated under increasing concentrations of antibiotic, and at days 1 and 12 for the
492 subinhibitory and non-antibiotic treatments. For the CIP-MICs, we used *Pseudomonas*
493 *aeruginosa* PAO1 in Mueller Hinton broth as a control. No differences in the MICs were
494 found between Mueller Hinton and $M9^+$ or if measuring the MIC in 96 well-plate or in 5
495 mL tubes, which are the experimental conditions. Each MIC was performed in triplicate.
496 The CIP was provided by Alfa Aesar (Alfa Aesar, Wardhill, MA). We also determined
497 the MIC of CIP in biofilm conditions adapting the method described by Diez-Aguilar to
498 the bead model (Díez-Aguilar et al., 2018). We resuspended each clone into fresh $M9^+$
499 containing sterile beads (as in the experimental evolution conditions, each tube used
500 contained three sterile beads and 5 mL of $M9^+$). After 24 hours growing at 37º, each bead
501 was propagated into new fresh $M9^+$ containing different CIP concentrations (from 4 to
502 128 mg/L in 2-fold-increasing manner). After 24 growing at 37º, we rinsed each bead in
503 PBS and sonicate them individually as explained before. 10 µl of the sonicated liquid

504 were transferred to 100 µL of $M9^+$. The MIC was calculated after measuring the optical
505 density at 650 nm before and after 24 hours incubation. The inhibition of growth was
506 defined as the lowest antibiotic that resulted in an OD difference at or below 0.05 after 6
507 hours of incubation.
508
509 We estimated the biofilm formation of the selected clones using a modification of the
510 previously described protocol (O'Toole & Kolter, 1998). We resurrected each clone in 5
511 mL of $M9^+$ containing 0.5 mg/L of CIP and grew them for 24 hours. For each strain, we
512 transferred 50 µl into 15 mL of $M9^+$. We tested 200 µl of the previous dilution of each
513 clone to 4 different subinhibitory CIP concentrations (0 mg/L, 0.01 mg/L, 0.03 mg/L and
514 0.0625 mg/L). After 24 hours of growing at 37ºC, we measured population sizes by
515 optical density (OD) at 590nm ($OD_{Populations}$). Then, we added 250 µl of 0.1% crystal violet
516 and incubated at room temperature for 15 minutes. After washing the wells and drying
517 for 24 hours, we added 250 µl 95% EtOH solution (95% EtOH, 4.95% dH2O, 0.05%
518 Triton X-100) to each well and incubated for 15 minutes and biofilm formation was
519 measured by the OD at 590nm ($OD_{Biofilm}$). Biofilm formation was corrected by population
520 sizes ($OD_{Biofilm}/OD_{Population}$). Results are the average of three experiments (Figure S3).
521
522 **Fitness measurement**
523 We selected 5 biofilm and 5 planktonic clones at the end of the evolutionary rescue
524 experiment (Figure 2) and determined the fitness by directly competing the ancestral
525 strain and the evolved clone variants both in planktonic and in biofilm conditions (Figure
526 3) (Turner et al., 2018). We revived each clone from a freezer stock in $M9^+$ for 24 hours.
527 We maintained the same evolutionary conditions to revive the clones, adding 3 beads
528 and/or CIP to the broth when required. After 24 hours, we added equal volume of the

529 clones and the ancestors in $M9^+$ in the absence of antibiotics. For planktonic populations,
530 we mixed 25 µl of each competitor in 5 mL of $M9^+$. For biofilm competitions, we
531 sonicated one bead per competitor in 1 mL of PBS and mixed in 5 mL of $M9^+$ containing
532 3 beads. The mix was cultured at 37ºC for 24 hours. We plated at time zero and after 24
533 hours. For each competition, we plated aliquots onto nonselective tryptic soy agar and
534 tryptic soy agar containing CIP. Selection rate (*r*) was calculated as the difference of the
535 Malthusian parameters for the two competitors: r = (ln(CIP $\text{resistant}_{d=1}$/CIP
536 $\text{resistant}_{d=0}$))/(ln(CIP $\text{susceptible}_{d=1}$/CIP $\text{susceptible}_{d=0}$))/day (Lenski, 1991). Susceptible
537 populations were calculated as the difference between the total populations (number of
538 colonies/mL growing on the nonselective plates) and the resistant fraction (number of
539 colonies/mL growing on the plates containing CIP). As a control for calculating the
540 correct ratio of susceptible vs. resistant populations, we replica plated 50 to 100 colonies
541 from the nonselective plates onto plates containing CIP as previously described (Santos-
542 Lopez et al., 2017). Results are the average of three to five independent experiments.
543
544 **Genome sequencing**
545 We sequenced whole populations of three evolving replicates per treatment. We
546 sequenced the populations at days 1, 3, 4, 6, 7, 9, 10, and 12 of the populations under
547 increasing concentrations of CIP (populations P1, P2, P3 and B1, B2, B3 for planktonic
548 and biofilm populations) and at days 1, 4, 9, and 12 of the populations under subinhibitory
549 concentration and no antibiotic treatments. In addition, we selected 49 clones for
550 sequencing at the end of the experiment (Figure 2F). 12 of the clones were recovered
551 from the populations propagated in the absence of the antibiotic, 12 clones from the
552 subinhibitory concentrations of CIP treatment and 25 were isolated from the increasing
553 concentrations of antibiotic. We revived each population or clone from a freezer stock in

554 the growth conditions under which they were isolated (*i.e.* the same CIP concentration
555 which they were exposed to during the experiment) and grew for 24 hours. DNA was
556 extracted using the Qiagen DNAeasy Blood and Tissue kit (Qiagen, Hiden, Germany).
557 The sequencing library was prepared as described by Turner and colleagues (Turner et
558 al., 2018) according to the protocol of Baym *et al.* (Baym et al., 2015), using the Illumina
559 Nextera kit (Illumina Inc., San Diego, CA) and sequenced using an Illumina NextSeq500
560 at the Microbial Genome Sequencing center (http://micropopbio.org/sequencing.html).
561

562 **Data processing**

563 All sequences were first quality filtered and trimmed with the Trimmomatic software
564 v0.36 (Bolger, Lohse, & Usadel, 2014) using the criteria: LEADING:20 TRAILING:20
565 SLIDINGWINDOW:4:20 MINLEN:70. Variants were called with the breseq software
566 v0.31.0 (Deatherage & Barrick, 2014) using the default parameters and the -p flag when
567 required for identifying polymorphisms in populations. This option calls a mutation if it
568 is observed in 2 reads from each strand and reaches 5% in the population. The average
569 depth of sequencing for populations was 219 $\pm$ 51x and average genome coverage was
570 98.7 $\pm$ 0.128%. The reference genome used for variant calling was downloaded from the
571 NCBI RefSeq database using the 17-Mar-2017 version of *A. baumannii* ATCC 17978-
572 mff complete genome (GCF_001077675.1). In addition to the chromosome
573 NZ_CP012004 and plasmid NZ_CP012005 sequences, we added two additional plasmid
574 sequences to the reference genome that are known to be present in our working strain of
575 *A. baumannii* ATCC 17978-mff: NC009083, NC_009084. Mutations were then manually
576 curated and filtered to remove false positives. Mutations were filtered if the gene was
577 found to contain a mutation when the ancestor sequence was compared to the reference
578 genome or if a mutation never reached a cumulative frequency of 10% across all replicate

579 populations. Diversity measurements were made in R using the Shannon index
580 considering the presence, absence, and frequency of alleles. Significant differences
581 between biofilm and planktonic populations were determined by the Kruskal Wallis test.
582 Filtering, mutational dynamics, and plotting were done in R v3.4.4 (www.r-project.org)
583 with the packages ggplot2 v2.2.1 (Wickham, 2016), dplyr v0.7.4 (Wickham, François,
584 Henry, & Müller, 2018), vegan v2.5-1 (Oksanen et al., 2018), and reshape2 (Wickham,
585 2007).
586
587 **Data Availability**
588 R code for filtering and data processing can be found here:
589 https://github.com/sirmicrobe/U01_allele_freq_code. All sequences were deposited into
590 NCBI under the Biosample accession numbers SAMN09783599-SAMN09783682.
591
592 **Authors contribution**
593 VSC, AS-L and CWM conceived and designed the study; AS-L and MRS performed the
594 experiments; DS sequenced the samples; CWM did the bioinformatic analysis; AS-L,
595 CWM and VSC wrote the paper.
596
597 **Acknowledgments**
598 We thank Caroline B. Turner for helpful discussions and proofreading of the paper,
599 Allison L. Welp for laboratory assistance and Christopher Deitrick for depositing the
600 sequences in the NCBI database. This research was supported by NIH U01AI124302-
601 01.

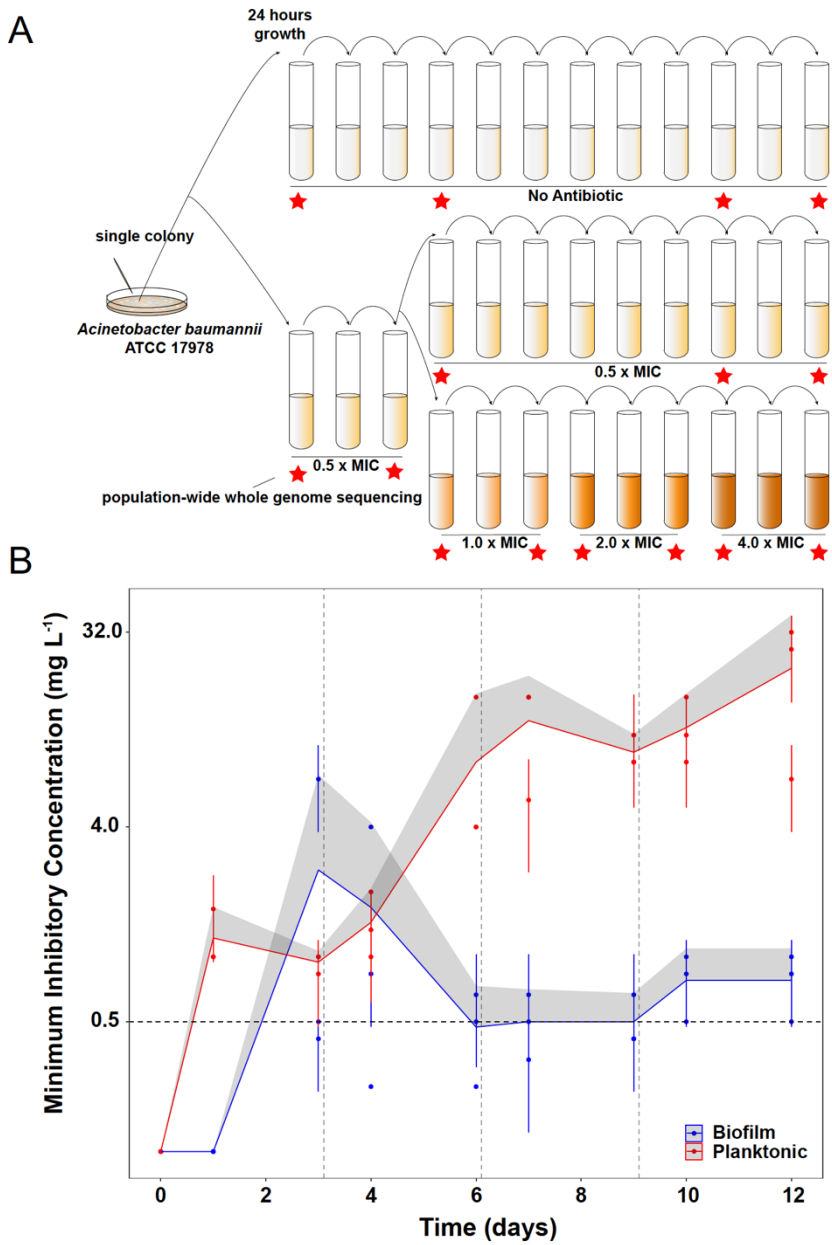

Figure 1. Experimental design (A) and dynamics of evolved resistance levels during the evolutionary rescue experiment (B).

A) A single clone of *A. baumannii* ATCC 17978 was propagated both in biofilm and planktonic conditions for 12 days under no antibiotics (top), subinhibitory concentrations of CIP (0.0625 mg/L = 0.5x MIC) (middle) or in increasing concentrations of CIP (bottom). For the latter, termed evolutionary rescue, the concentration of CIP was doubled from 0.5 x MIC to 4.0 x MIC every 72 hours. As a control, five populations of *A.*

610 *baumannii* ATCC 17978 were propagated in biofilm and five in planktonic conditions in
611 the absence of antibiotics. We estimated the MICs to CIP and froze the populations for
612 sequencing before and after doubling the antibiotic concentrations (red stars). B) MICs
613 (mg/L) of CIP were measured for replicate populations during the evolutionary rescue.
614 The red and blue points represent the MICs of three populations propagated in planktonic
615 or biofilm, respectively, with the 95% CI represented by the error bars. The red and blue
616 lines represent the grand mean of the three planktonic and biofilm populations,
617 respectively, with the upper 95% CI indicated by the grey shaded area. Horizontal dashed
618 line indicates the highest CIP exposure during the experiment (4x MIC) and vertical lines
619 indicate time when CIP concentration was doubled.

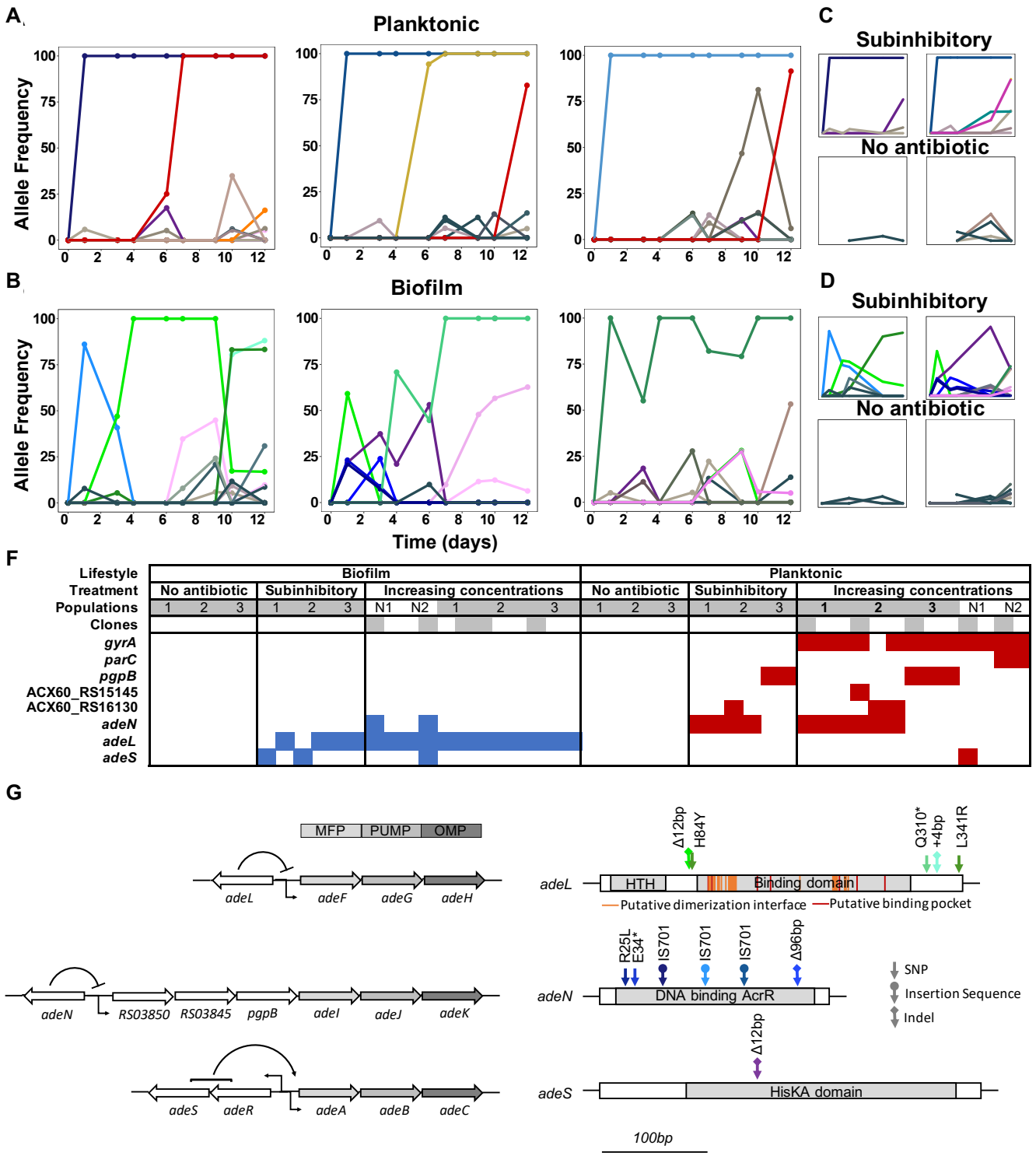

620

621 **Figure 2. Lifestyle-dependent mutations and dynamics under increasing CIP**

622 **selection.**

623 Mutation frequencies in planktonic (A and C) and biofilm populations (B and D) over

624 time as determined by population-wide whole genome sequencing. A) and B) show the

625 mutation frequencies obtained under increasing concentrations of CIP. From left to right:
626 P1, P2 and P3 in A) and B1, B2 and B3 in B). C) and D) show the mutation frequencies
627 obtained under the subinhibitory (top) and no antibiotic (bottom) treatments. Mutations
628 in the same gene share a color. Blue: *adeN* or genes regulated by *adeN*; green: *adeL*; gold:
629 MFS putative transporter ACX60_RS15145; purple: *adeS*; pink: *sohB*; red: *gyrA;* and
630 orange: *parC*. Grey and brown colors indicate genes potentially unrelated to adaptation
631 to CIP. F) Mutated genes in the sequenced clones. Each column represents one clone.
632 Grey shading of populations indicates whole population sequencing and N1 and N2
633 indicate populations where only clones were sequenced. Grey shaded clones were used
634 for MIC and fitness estimations. Blue and red indicate SNPs in biofilm and planktonic
635 growing populations respectively. For all SNPs identified in the 49 clones, see Figure S2
636 and Table S6. G) The genetic organization of the RND efflux pumps is shown on the left.
637 MFP and OMP denote membrane fusion protein and outer membrane protein
638 respectively. All mutations found in the RND regulators are shown on the right.

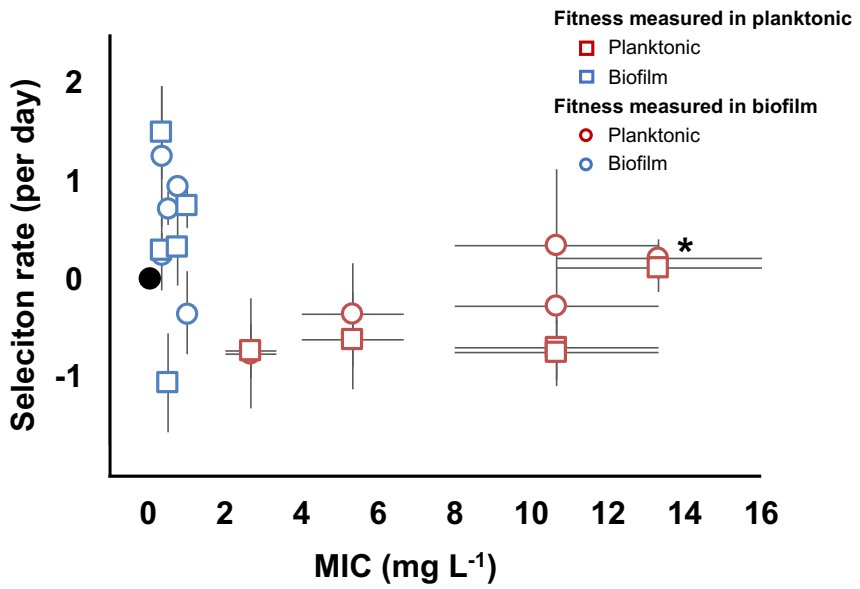

639

640 **Figure 3. Evolved trade-off between resistance level and fitness.**

641 Relative fitness (average ± SEM) of 10 evolved clones from the evolutionary rescue

642 experiment compared to the ancestor and their MICs (mg/L) to CIP. Fitness was measured

643 in both planktonic (squares) and biofilm (circles) conditions. MICs were estimated in

644 planktonic conditions. Black dot represents the ancestral clone. *Denotes the clone with

645 *gyrA* and *parC* mutations.

646

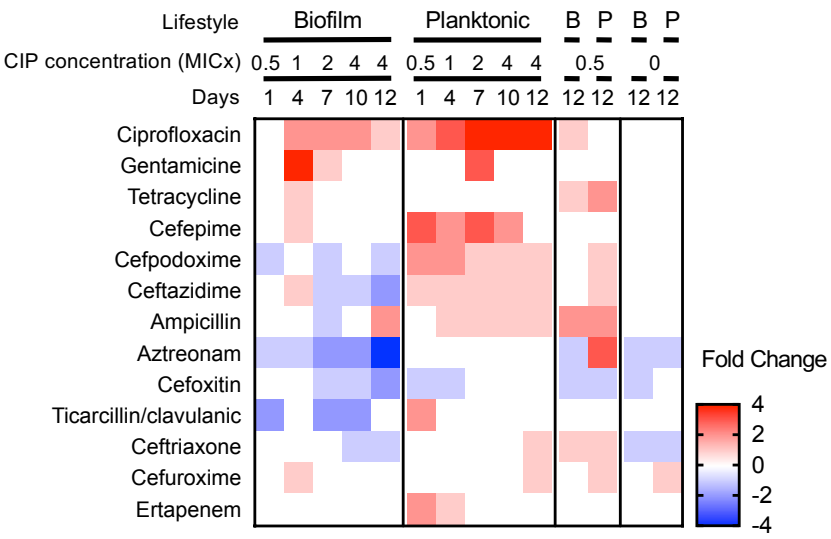

Figure 4. Collateral sensitivities and cross resistances to various antibiotics. Heat map showing the relative changes in antimicrobial susceptibility to 13 of the 23 antibiotics tested in the evolved populations (those not shown had no changes). Results shown are the median values of the fold change in the evolved populations compared to the ancestral strain. For subinhibitory and no-antibiotic treatments, only day 12 is shown.

	Increasing concentrations		Subinhibitory concentrations	
	Planktonic	**Biofilm**	**Planktonic**	**Biofilm**
Total mutations	30	40	6	16
Nonsynonymous/Synonymous[b]	8.5	9.67	2/0	6
Intergenic	8	11	0	4
Nonsynonymous	9	13	2	6
Percent intergenic mutations[b]	0.32	0.29	0	0.25

652

653 **Table 1. Mutation spectrum of different selective environments.** Attributes of the
654 contending mutations during the 12 days of the evolution experiment. [a]Results from the
655 last day of the experimental evolution. [b]Accounting for all unique mutations detected after
656 filtering (see methods). For mutation dynamics over time, see Table S3.

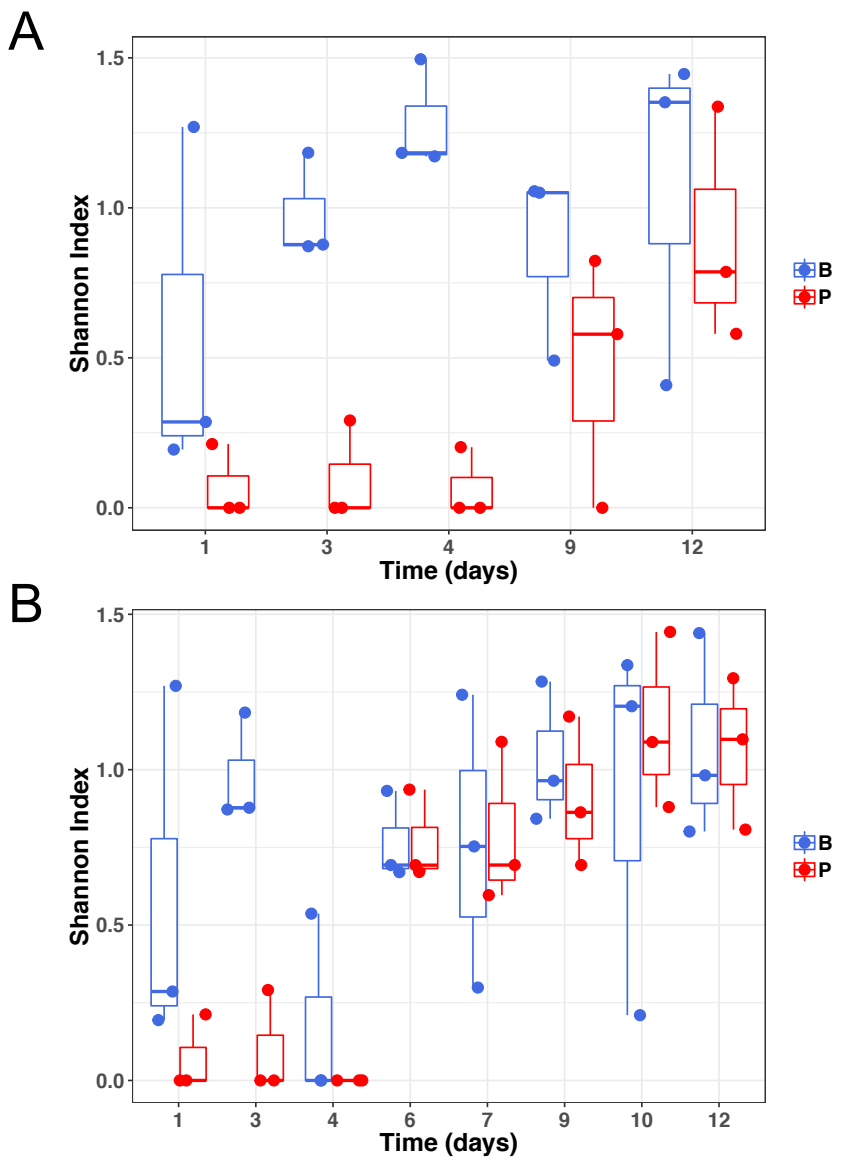

657

658 **Figure S1. Genetic diversity of samples at subinhibitory concentrations of**

659 **ciprofloxacin (A) or during the evolutionary rescue experiment with increasing**

660 **concentrations of ciprofloxacin (B).** Biofilm populations in blue and planktonic

661 populations in red.

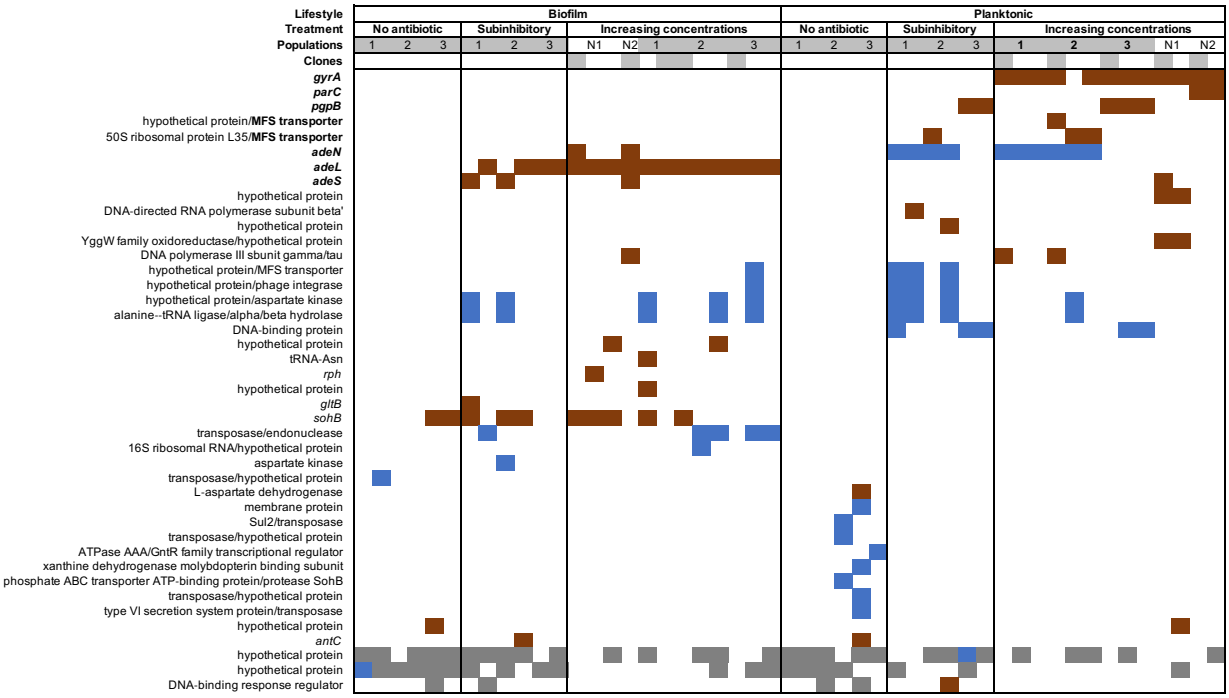

Figure S2. Mutated genes in the sequenced clones differ between treatments. Each column represents one clone. Grey shaded clones were used for MIC and fitness estimations. Red color indicates SNPs or small indels, blue color indicates new junction evidences and grey indicates missing coverage indicative of a deletion.

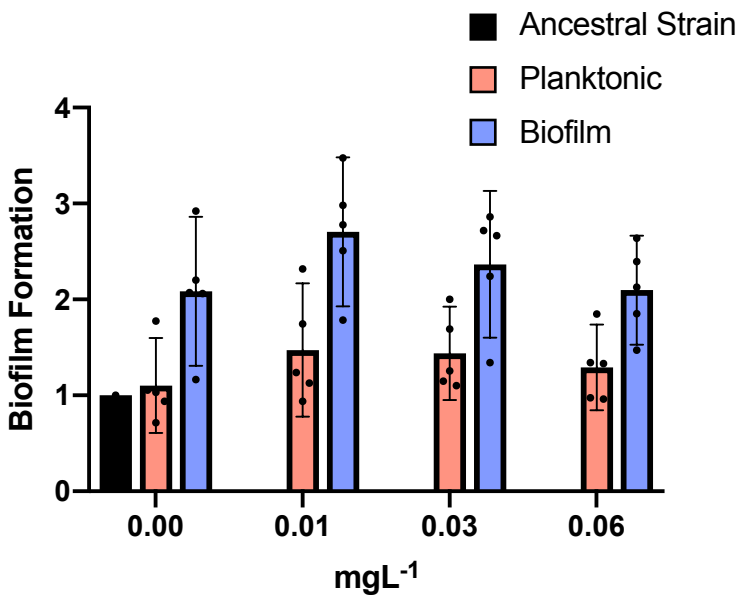

667

668 **Figure S3. Biofilm production under subinhibitory concentrations of CIP.** Blue and
669 red bars show biofilm and planktonic clones, respectively. The ancestral strain is
670 represented by the black bar. Individual clone results are shown as points. The averages
671 are shown by bars. 95% CI are indicated by the error bars. Biofilm clones produced more
672 biofilm than planktonic clones: two tailed t-test of biofilm formation with 0.00 mg/L of
673 CIP: $p = 0.006$, $t = 3.008$, $df = 32$; with 0.01 mg/L of CIP: $p = 0.0006$, $t = 3.780$, $df = 32$;
674 with 0.03 mg/L of CIP: $p = 0.0077$ $t = 2.841$, $df = 32$ and with 0.0625 mg/L of CIP: $p =$
675 0.018 $t = 2.471$ $df = 32$.

676

Treatment and Populations		MIC (mg/L)	Fold MIC increase
No Antibiotic			
Planktonic			
	P1	0.25 ± 0.00	2
	P2	0.25 ± 0	2
	P3	0.21 ± 0.03	1.68
Biofilm			
	B1	0.25 ± 0	2
	B2	0.25 ± 0	2
	B3	0.25 ± 0	2
Subinhibitory			
Planktonic			
	P1	2.33 ± 0.72	18.64
	P2	4 ± 0	32
	P3	1 ± 0	8
Biofilm			
	B1	0.41 ± 0.07	3.28
	B2	0.5 ± 0	4
	B3	0.5 ± 0	4
Evolutionary rescue			
Planktonic			
	P1	26.67 ± 5.34	213.36
	P2	32 ± 0	256
	P3	6.67 ± 1.34	53.36
Biofilm			
	B1	1 ± 0	8
	B2	0.5 ± 0	4
	B3	0.83 ± 0.17	6.64

677

678 **Table S1. Antibiotic susceptibility of the populations propagated in the absence, in**
679 **subinhibitory concentrations or increasing concentrations of CIP at the end of the**
680 **experiment (day 12).** MICs are expressed in mg/L and standard errors of the mean are
681 indicated. Fold increase in MIC compared to the ancestral strain are also indicated.

Treatment and Populations	MIC measured in biofilms (mg/L)	Fold MIC increase
Evolutionary rescue		
Planktonic		
P1	> 128 ± 0	>1024
P2	> 128 ± 0	>1024
P3	> 128 ± 0	>1024
Biofilm		
B1	32 ± 0	256
B2	32 ± 0	256
B3	32 ± 0	256

682

683 **Table S2. Antibiotic susceptibility of one clone of each population propagated in**

684 **increasing concentrations of CIP at the end of the experiment (day 12).** MICs were

685 measured in biofilms and are expressed in mg/L and standard errors of the mean are

686 indicated. Fold increase in MIC compared to the ancestral strain are also indicated.

687 **Table S3. Mutation probabilities (attached XLS file)**

688

		Increasing concentrations				Subinhibitory concentrations			
	Days	**Nonsynonymous/Synonymous**	**Intergenic mutations**	**Structural variants**	**Total mutations**	**Nonsynonymous/Synonymous**	**Intergenic mutations**	**Structural variants**	**Total mutations**
Biofilm	1	4/0	0	4	8	4/0	0	4	8
	3	5/0	0	8	13	5/0	0	8	13
	4	2/0	0	2	4	6/1	2	8	17
	6	3/1	0	4	8	-	-	-	-
	7	6/0	3	4	10	-	-	-	-
	9	5/0	2	6	11	4/0	1	6	11
	10	7/0	2	5	12	-	-	-	-
	12	7/0	1	6	13	5/0	1	7	12
Planktonic	1	1/0	0	3	4	1/0	0	3	4
	3	2/0	0	2	4	2/0	0	2	4
	4	1/0	0	2	3	1/0	0	3	4
	6	5/0	2	7	12	-	-	-	-
	7	6/0	3	4	10	-	-	-	-
	9	3/1	3	6	10	2/0	1	4	7
	10	5/2	5	6	13	-	-	-	-
	12	7/1	1	5	13	2/0	2	7	11

689 **Table S4. Attributes of the contending mutations each day in the experimental**

690 **evolution.**

Locus Tag	Mutation	Annotation	Description
ACX60_RS01385	A→G	E292G (GAG→GGG)	energy-dependent translational throttle protein EttA
ACX60_RS04575	C→T	R226H (CGT→CAT)	fructose 1,6-bisphosphatase
ACX60_RS18160	(ATGGTG)9→8	coding (454-459/987 nt)	cation transporter

691

692 **Table S5. Mutated genes in the ancestral strain compared to the *A. baumannii***

693 **ATCC 17978-mff complete genome (GCF_001077675.1) after 10 days of evolution**

694 **in M9^{+}.**

695

696 **Table S6. Complete list of mutated genes from the sequenced clones (attached XLS**

697 **file)**

Transporter Family	Regulator	Efflux pump	Substrates[a]
RND	AdeSR	AdeABC	AG, **BL**, CHL, ERY, **FQ**, NAL, TET, TGC
RND	AdeL	AdeFGH	CHL, ERY, **FQ**, NAL, SUL, TET, TGC, TMP
RND	AdeN	AdeIJK	AZI, **BL**, CHL, ERY, **FQ**, FUA, MIN, NAL, RIF, SA, SUL, TET, TMP
MATE	-	AbeM	**FQ**, GEN

698

699 **Table S7. Efflux pumps and their regulators in *A. baumannii* 17978 targeted under**
700 **CIP pressure.** Table adapted from (Li, Elkins et al. 2016). AG aminoglycosides, AZI
701 azithromycin, BL β-lactams, CHL chloramphenicol, CIP CIP, CL clindamycin, ERY
702 erythromycin, FLO florfenicol, FUA fusidic acid, GEN gentamicin, MIN minocycline,
703 NAL nalidixic acid, NOR norfloxacin, RIF rifampicin, SUL sulfonamides, TET
704 tetracycline, TGC tigecycline, TMP trimethoprim. [a] References in (X.-Z. Li et al., 2016).

References

Adams-Haduch, J. M., Paterson, D. L., Sidjabat, H. E., Pasculle, A. W., Potoski, B. A., Muto, C. A., . . . Doi, Y. (2008). Genetic basis of multidrug resistance in Acinetobacter baumannii clinical isolates at a tertiary medical center in Pennsylvania. *Antimicrob Agents Chemother, 52*(11), 3837-3843. doi:10.1128/aac.00570-08

Ahmed, M. N., Porse, A., Sommer, M. O. A., Hoiby, N., & Ciofu, O. (2018). Evolution of antibiotic resistance in biofilm and planktonic P. aeruginosa populations exposed to sub-inhibitory levels of ciprofloxacin. *Antimicrob Agents Chemother*. doi:10.1128/aac.00320-18

Aka, S. T., & Haji, S. H. (2015). Sub-MIC of antibiotics induced biofilm formation of Pseudomonas aeruginosa in the presence of chlorhexidine. *Braz J Microbiol, 46*(1), 149-154. doi:10.1590/S1517-838246120140218

Alav, I., Sutton, J. M., & Rahman, K. M. (2018). Role of bacterial efflux pumps in biofilm formation. *J Antimicrob Chemother, 73*(8), 2003-2020. doi:10.1093/jac/dky042

Andersson, D. I., & Hughes, D. (2014). Microbiological effects of sublethal levels of antibiotics. *Nat Rev Microbiol, 12*(7), 465-478. doi:10.1038/nrmicro3270

Ardebili, A., Lari, A. R., & Talebi, M. (2014). Correlation of ciprofloxacin resistance with the AdeABC efflux system in Acinetobacter baumannii clinical isolates. *Ann Lab Med, 34*(6), 433-438. doi:10.3343/alm.2014.34.6.433

Asif, M., Alvi, I. A., & Rehman, S. U. (2018). Insight into Acinetobacter baumannii: pathogenesis, global resistance, mechanisms of resistance, treatment options, and alternative modalities. *Infect Drug Resist, 11*, 1249-1260. doi:10.2147/idr.S166750

Azimi, L., & Rastegar Lari, A. (2017). Collateral sensitivity between aminoglycosides and beta-lactam antibiotics depends on active proton pumps. *Microb Pathog, 112*, 122-125. doi:10.1016/j.micpath.2017.09.049

Baquero, F., Negri, M. C., Morosini, M. I., & Blazquez, J. (1998). Antibiotic-selective environments. *Clin Infect Dis, 27 Suppl 1*, S5-11.

Barbosa, C., Trebosc, V., Kemmer, C., Rosenstiel, P., Beardmore, R., Schulenburg, H., & Jansen, G. (2017). Alternative Evolutionary Paths to Bacterial Antibiotic Resistance Cause Distinct Collateral Effects. *Mol Biol Evol, 34*(9), 2229-2244. doi:10.1093/molbev/msx158

Barrick, J. E., & Lenski, R. E. (2013). Genome dynamics during experimental evolution. *Nature reviews. Genetics, 14*, 827-839. doi:10.1038/nrg3564

Barrick, J. E., Yu, D. S., Yoon, S. H., Jeong, H., Oh, T. K., Schneider, D., . . . Kim, J. F. (2009). Genome evolution and adaptation in a long-term experiment with Escherichia coli. *Nature, 461*, 1243-1247. doi:10.1038/nature08480

Basra, P., Alsaadi, A., Bernal-Astrain, G., O'Sullivan, M. L., Hazlett, B., Clarke, L. M., . . . Wong, A. (2018). Fitness tradeoffs of antibiotic resistance in extra-intestinal pathogenic Escherichia coli. *Genome Biol Evol*. doi:10.1093/gbe/evy030

Baumann, P., Doudoroff, M., & Stanier, R. Y. (1968). A study of the Moraxella group. II. Oxidative-negative species (genus Acinetobacter). *J Bacteriol, 95*(5), 1520-1541.

Baym, M., Kryazhimskiy, S., Lieberman, T. D., Chung, H., Desai, M. M., & Kishony, R. (2015). Inexpensive multiplexed library preparation for megabase-sized genomes. *PLoS One, 10*(5), e0128036. doi:10.1371/journal.pone.0128036

Baym, M., Lieberman, T. D., Kelsic, E. D., Chait, R., Gross, R., Yelin, I., & Kishony, R. (2016). Spatiotemporal microbial evolution on antibiotic landscapes. *Science, 353*(6304), 1147-1151. doi:10.1126/science.aag0822

Baym, M., Stone, L. K., & Kishony, R. (2016). Multidrug evolutionary strategies to reverse antibiotic resistance. *Science, 351*(6268), aad3292. doi:10.1126/science.aad3292

Bell, G., & Gonzalez, A. (2009). Evolutionary rescue can prevent extinction following environmental change. *Ecol Lett, 12*(9), 942-948. doi:10.1111/j.1461-0248.2009.01350.x

Bolger, A. M., Lohse, M., & Usadel, B. (2014). Trimmomatic: a flexible trimmer for Illumina sequence data. *Bioinformatics, 30*(15), 2114-2120. doi:10.1093/bioinformatics/btu170

Bolnick, D. I., Barrett, R. D. H., Oke, K. B., Rennison, D. J., & Stuart, Y. E. (2018). (Non)Parallel Evolution. *Annual Review of Ecology, Evolution, and Systematics, 49*(1), 303-330. doi:10.1146/annurev-ecolsys-110617-062240

Borriello, G., Werner, E., Roe, F., Kim, A. M., Ehrlich, G. D., & Stewart, P. S. (2004). Oxygen limitation contributes to antibiotic tolerance of Pseudomonas aeruginosa in biofilms. *Antimicrob Agents Chemother, 48*(7), 2659-2664. doi:10.1128/aac.48.7.2659-2664.2004

Brockhurst, M. A., Harrison, F., Veening, J. W., Harrison, E., Blackwell, G., Iqbal, Z., & Maclean, C. (2019). Assessing evolutionary risks of resistance for new antimicrobial therapies. *Nat Ecol Evol, 3*(4), 515-517. doi:10.1038/s41559-019-0854-x

CLSI. (2017). CLSI. Clinical and Laboratory Standars Institute. Performance Standards for Antimicrobial Susceptibility Testing-Seventeenth edition: Approved Standar M100-S17. Wayne, PA, USA: CLSI.

Cooper, V. S. (2018). Experimental Evolution as a High-Throughput Screen for Genetic Adaptations. *mSphere, 3*(3). doi:10.1128/mSphere.00121-18

Cooper, V. S., Staples, R. K., Traverse, C. C., & Ellis, C. N. (2014). Parallel evolution of small colony variants in Burkholderia cenocepacia biofilms. *Genomics, 104*(6 Pt A), 447-452. doi:10.1016/j.ygeno.2014.09.007

Coyne, S., Courvalin, P., & Perichon, B. (2011). Efflux-mediated antibiotic resistance in Acinetobacter spp. *Antimicrob Agents Chemother, 55*(3), 947-953. doi:10.1128/aac.01388-10

Coyne, S., Rosenfeld, N., Lambert, T., Courvalin, P., & Perichon, B. (2010). Overexpression of resistance-nodulation-cell division pump AdeFGH confers multidrug resistance in Acinetobacter baumannii. *Antimicrob Agents Chemother, 54*(10), 4389-4393. doi:10.1128/AAC.00155-10

Dahdouh, E., Gomez-Gil, R., Pacho, S., Mingorance, J., Daoud, Z., & Suarez, M. (2017). Clonality, virulence determinants, and profiles of resistance of clinical Acinetobacter baumannii isolates obtained from a Spanish hospital. *PLoS One, 12*(4), e0176824. doi:10.1371/journal.pone.0176824

Damier-Piolle, L., Magnet, S., Bremont, S., Lambert, T., & Courvalin, P. (2008). AdeIJK, a resistance-nodulation-cell division pump effluxing multiple antibiotics in Acinetobacter baumannii. *Antimicrob Agents Chemother, 52*(2), 557-562. doi:10.1128/AAC.00732-07

de Visser, J. A., & Rozen, D. E. (2006). Clonal interference and the periodic selection of new beneficial mutations in Escherichia coli. *Genetics, 172*(4), 2093-2100. doi:10.1534/genetics.105.052373

Deatherage, D. E., & Barrick, J. E. (2014). Identification of mutations in laboratory-evolved microbes from next-generation sequencing data using breseq. *Methods Mol Biol, 1151*, 165-188. doi:10.1007/978-1-4939-0554-6_12

Dhawan, A., Nichol, D., Kinose, F., Abazeed, M. E., Marusyk, A., Haura, E. B., & Scott, J. G. (2017). Collateral sensitivity networks reveal evolutionary instability and novel treatment strategies in ALK mutated non-small cell lung cancer. *Sci Rep, 7*(1), 1232. doi:10.1038/s41598-017-00791-8

Díez-Aguilar, M., Morosini, M. I., Köksal, E., Oliver, A., Ekkelenkamp, M., & Cantón, R. (2018). Use of Calgary and Microfluidic BioFlux Systems To Test the Activity of Fosfomycin and Tobramycin Alone and in Combination against Cystic Fibrosis Pseudomonas aeruginosa Biofilms. *Antimicrobial agents and chemotherapy, 62*(1), e01650-01617. doi:10.1128/aac.01650-17

Dillon, M. M., Sung, W., Sebra, R., Lynch, M., & Cooper, V. S. (2017). Genome-Wide Biases in the Rate and Molecular Spectrum of Spontaneous Mutations in Vibrio cholerae and Vibrio fischeri. *Mol Biol Evol, 34*(1), 93-109. doi:10.1093/molbev/msw224

Doi, Y., Murray, G. L., & Peleg, A. Y. (2015). Acinetobacter baumannii: evolution of antimicrobial resistance-treatment options. *Semin Respir Crit Care Med, 36*(1), 85-98. doi:10.1055/s-0034-1398388

Elena, S. F., & Lenski, R. E. (2003). Evolution experiments with microorganisms: the dynamics and genetic bases of adaptation. *Nature Reviews Genetics, 4*, 457. doi:10.1038/nrg1088

Ellis, C. N., Traverse, C. C., Mayo-Smith, L., Buskirk, S. W., & Cooper, V. S. (2015). Character displacement and the evolution of niche complementarity in a model biofilm community. *Evolution, 69*(2), 283-293. doi:10.1111/evo.12581

Eze, E. C., Chenia, H. Y., & El Zowalaty, M. E. (2018). Acinetobacter baumannii biofilms: effects of physicochemical factors, virulence, antibiotic resistance determinants, gene regulation, and future antimicrobial treatments. *Infect Drug Resist, 11*, 2277-2299. doi:10.2147/idr.S169894

Fernando, D., Zhanel, G., & Kumar, A. (2013). Antibiotic resistance and expression of resistance-nodulation-division pump- and outer membrane porin-encoding genes in Acinetobacter species isolated from Canadian hospitals. *Can J Infect Dis Med Microbiol, 24*(1), 17-21.

France, M. T., Cornea, A., Kehlet-Delgado, H., & Forney, L. J. (2019). Spatial structure facilitates the accumulation and persistence of antibiotic-resistant mutants in biofilms. *Evolutionary Applications, 12*(3), 498-507. doi:doi:10.1111/eva.12728

Fux, C. A., Costerton, J. W., Stewart, P. S., & Stoodley, P. (2005). Survival strategies of infectious biofilms. *Trends Microbiol, 13*(1), 34-40. doi:10.1016/j.tim.2004.11.010

Geisinger, E., & Isberg, R. R. (2015). Antibiotic modulation of capsular exopolysaccharide and virulence in Acinetobacter baumannii. *PLoS Pathog, 11*(2), e1004691. doi:10.1371/journal.ppat.1004691

Geisinger, E., Vargas-Cuebas, G., Mortman, N. J., Syal, S., Wainwright, E., Lazinski, D. W., . . . Isberg, R. R. (2018). The landscape of intrinsic and evolved fluoroquinolone resistance in Acinetobacter baumannii includes suppression of drug-induced prophage replication. *bioRxiv*, 442681. doi:10.1101/442681

Habets, M. G., Rozen, D. E., Hoekstra, R. F., & de Visser, J. A. (2006). The effect of population structure on the adaptive radiation of microbial populations evolving in spatially structured environments. *Ecol Lett, 9*(9), 1041-1048. doi:10.1111/j.1461-0248.2006.00955.x

Hamed, K., & Debonnett, L. (2017). Tobramycin inhalation powder for the treatment of pulmonary Pseudomonas aeruginosa infection in patients with cystic fibrosis: a review based on clinical evidence. *Ther Adv Respir Dis, 11*(5), 193-209. doi:10.1177/1753465817691239

He, X., Lu, F., Yuan, F., Jiang, D., Zhao, P., Zhu, J., . . . Lu, G. (2015). Biofilm Formation Caused by Clinical Acinetobacter baumannii Isolates Is Associated with Overexpression of the AdeFGH Efflux Pump. *Antimicrob Agents Chemother, 59*(8), 4817-4825. doi:10.1128/AAC.00877-15

Hill, D., Rose, B., Pajkos, A., Robinson, M., Bye, P., Bell, S., . . . Harbour, C. (2005). Antibiotic Susceptibilities of Pseudomonas aeruginosa Isolates Derived from Patients with Cystic Fibrosis under Aerobic, Anaerobic, and Biofilm Conditions. *Journal of Clinical Microbiology, 43*(10), 5085-5090. doi:10.1128/jcm.43.10.5085-5090.2005

Hoffman, L. R., D'Argenio, D. A., MacCoss, M. J., Zhang, Z., Jones, R. A., & Miller, S. I. (2005). Aminoglycoside antibiotics induce bacterial biofilm formation. *Nature, 436*(7054), 1171-1175. doi:10.1038/nature03912

Hoiby, N., Bjarnsholt, T., Givskov, M., Molin, S., & Ciofu, O. (2010). Antibiotic resistance of bacterial biofilms. *Int J Antimicrob Agents, 35*(4), 322-332. doi:10.1016/j.ijantimicag.2009.12.011

Hua, X., Chen, Q., Li, X., & Yu, Y. (2014). Global transcriptional response of Acinetobacter baumannii to a subinhibitory concentration of tigecycline. *Int J Antimicrob Agents, 44*(4), 337-344. doi:10.1016/j.ijantimicag.2014.06.015

Hughes, D., & Andersson, D. I. (2017). Evolutionary Trajectories to Antibiotic Resistance. *Annu Rev Microbiol*. doi:10.1146/annurev-micro-090816-093813

Huseby, D. L., Pietsch, F., Brandis, G., Garoff, L., Tegehall, A., & Hughes, D. (2017). Mutation Supply and Relative Fitness Shape the Genotypes of Ciprofloxacin-Resistant Escherichia coli. *Mol Biol Evol, 34*(5), 1029-1039. doi:10.1093/molbev/msx052

Imamovic, L., & Sommer, M. O. (2013). Use of collateral sensitivity networks to design drug cycling protocols that avoid resistance development. *Sci Transl Med, 5*(204), 204ra132. doi:10.1126/scitranslmed.3006609

Kassen, R. (2009). Toward a general theory of adaptive radiation: insights from microbial experimental evolution. *Ann N Y Acad Sci, 1168*, 3-22. doi:10.1111/j.1749-6632.2009.04574.x

Khan, G. A., Berglund, B., Khan, K. M., Lindgren, P. E., & Fick, J. (2013). Occurrence and abundance of antibiotics and resistance genes in rivers, canal and near drug formulation facilities--a study in Pakistan. *PLoS One, 8*(6), e62712. doi:10.1371/journal.pone.0062712

Kim, S., Lieberman, T. D., & Kishony, R. (2014). Alternating antibiotic treatments constrain evolutionary paths to multidrug resistance. *Proc Natl Acad Sci U S A, 111*(40), 14494-14499. doi:10.1073/pnas.1409800111

Kirby, A. E., Garner, K., & Levin, B. R. (2012). The relative contributions of physical structure and cell density to the antibiotic susceptibility of bacteria in biofilms. *Antimicrob Agents Chemother, 56*(6), 2967-2975. doi:10.1128/AAC.06480-11

Kröger, C., MacKenzie, K. D., Alshabib, E. Y., Kirzinger, M. W. B., Suchan, D. M., Chao, T. C., . . . Cameron, A. D. S. (2018). The primary transcriptome, small RNAs and regulation of antimicrobial resistance in Acinetobacter baumannii ATCC 17978. *Nucleic Acids Res, 46*(18), 9684-9698. doi:10.1093/nar/gky603

Kugelberg, E., Lofmark, S., Wretlind, B., & Andersson, D. I. (2005). Reduction of the fitness burden of quinolone resistance in Pseudomonas aeruginosa. *J Antimicrob Chemother, 55*(1), 22-30. doi:10.1093/jac/dkh505

Lenski, R. E. (1991). Quantifying fitness and gene stability in microorganisms. *Biotechnology, 15*, 173-192.

Leus, I. V., Weeks, J. W., Bonifay, V., Smith, L., Richardson, S., & Zgurskaya, H. I. (2018). Substrate specificities and efflux efficiencies of RND efflux pumps of Acinetobacter baumannii. *J Bacteriol*. doi:10.1128/JB.00049-18

Li, X.-Z., Elkins, C. A., & Zgurskaya, H. I. (2016). *Efflux-Mediated Antimicrobial Resistance in Bacteria: Mechanisms, Regulation and Clinical Implications*: Springer.

Linares, J. F., Gustafsson, I., Baquero, F., & Martinez, J. L. (2006). Antibiotics as intermicrobial signaling agents instead of weapons. *Proc Natl Acad Sci U S A, 103*(51), 19484-19489. doi:10.1073/pnas.0608949103

Lopes, B. S., & Amyes, S. G. (2013). Insertion sequence disruption of adeR and ciprofloxacin resistance caused by efflux pumps and gyrA and parC mutations in Acinetobacter baumannii. *Int J Antimicrob Agents, 41*(2), 117-121. doi:10.1016/j.ijantimicag.2012.08.012

Lynch, M., Ackerman, M. S., Gout, J.-F., Long, H., Sung, W., Thomas, W. K., & Foster, P. L. (2016). Genetic drift, selection and the evolution of the mutation rate. *Nature Reviews Genetics, 17*, 704. doi:10.1038/nrg.2016.104

Maclean, R. C., Hall, A. R., Perron, G. G., & Buckling, A. (2010). The evolution of antibiotic resistance: insight into the roles of molecular mechanisms of resistance and treatment context. *Discov Med, 10*(51), 112-118.

Marcusson, L. L., Frimodt-Moller, N., & Hughes, D. (2009). Interplay in the selection of fluoroquinolone resistance and bacterial fitness. *PLoS Pathog, 5*(8), e1000541. doi:10.1371/journal.ppat.1000541

Martínez, J. L. (2008). Antibiotics and Antibiotic Resistance Genes in Natural Environments. *Science, 321*(5887), 365-367. doi:10.1126/science.1159483

Moore, F. B., Rozen, D. E., & Lenski, R. E. (2000). Pervasive compensatory adaptation in Escherichia coli. *Proc Biol Sci, 267*(1442), 515-522. doi:10.1098/rspb.2000.1030

Nichol, D., Rutter, J., Bryant, C., Hujer, A. M., Lek, S., Adams, M. D., . . . Scott, J. G. (2019). Antibiotic collateral sensitivity is contingent on the repeatability of evolution. *Nature Communications, 10*(1), 334. doi:10.1038/s41467-018-08098-6

O'Toole, G. A., & Kolter, R. (1998). Initiation of biofilm formation in Pseudomonas fluorescens WCS365 proceeds via multiple, convergent signalling pathways: a genetic analysis. *Mol Microbiol, 28*(3), 449-461.

O´Neill, J. (2016). TACKLING DRUG-RESISTANT INFECTIONS GLOBALLY: FINAL REPORT AND RECOMMENDATIONS. *Review on Antimicrobal Resistance*.

Oksanen, J., Blanchet, F. G., Friendly, M., Kindt, R., Pierre Legendre, McGlinn, D., . . . Wagner, H. (2018). Vegan: Community Ecology Package. R package version 2.5-3. https://CRAN.R-project.org/package=vegan.

Olivares Pacheco, J., Alvarez-Ortega, C., Alcalde Rico, M., & Martínez, J. L. (2017). Metabolic Compensation of Fitness Costs Is a General Outcome for Antibiotic-Resistant Pseudomonas aeruginosa Mutants Overexpressing Efflux Pumps. *MBio, 8*(4), e00500-00517. doi:10.1128/mBio.00500-17

Olsen, I. (2015). Biofilm-specific antibiotic tolerance and resistance. *Eur J Clin Microbiol Infect Dis, 34*(5), 877-886. doi:10.1007/s10096-015-2323-z

Oz, T., Guvenek, A., Yildiz, S., Karaboga, E., Tamer, Y. T., Mumcuyan, N., . . . Toprak, E. (2014). Strength of selection pressure is an important parameter contributing to the complexity of antibiotic resistance evolution. *Mol Biol Evol, 31*(9), 2387-2401. doi:10.1093/molbev/msu191

Pal, C., Papp, B., & Lazar, V. (2015). Collateral sensitivity of antibiotic-resistant microbes. *Trends Microbiol, 23*(7), 401-407. doi:10.1016/j.tim.2015.02.009

Piechaud, M., & Second, L. (1951). [Studies of 26 strains of Moraxella Iwoffi]. *Ann Inst Pasteur (Paris), 80*(1), 97-99.

Podnecky, N. L., Fredheim, E. G. A., Kloos, J., Sørum, V., Primicerio, R., Roberts, A. P., . . . Johnsen, P. J. (2018). Conserved collateral antibiotic susceptibility networks in diverse clinical strains of Escherichia coli. *Nature Communications, 9*(1), 3673. doi:10.1038/s41467-018-06143-y

Poltak, S. R., & Cooper, V. S. (2011). Ecological succession in long-term experimentally evolved biofilms produces synergistic communities. *ISME J, 5*(3), 369-378. doi:10.1038/ismej.2010.136

Pournaras, S., Koumaki, V., Gennimata, V., Kouskouni, E., & Tsakris, A. (2016). In Vitro Activity of Tigecycline Against Acinetobacter baumannii: Global Epidemiology and Resistance Mechanisms. *Adv Exp Med Biol, 897*, 1-14. doi:10.1007/5584_2015_5001

Ridenhour, B. J., Metzger, G. A., France, M., Gliniewicz, K., Millstein, J., Forney, L. J., & Top, E. M. (2017). Persistence of antibiotic resistance plasmids in bacterial biofilms. *Evol Appl, 10*(6), 640-647. doi:10.1111/eva.12480

Rosenfeld, N., Bouchier, C., Courvalin, P., & Perichon, B. (2012). Expression of the resistance-nodulation-cell division pump AdeIJK in Acinetobacter baumannii is regulated by AdeN, a TetR-type regulator. *Antimicrob Agents Chemother, 56*(5), 2504-2510. doi:10.1128/AAC.06422-11

Sackman, A. M., & Rokyta, D. R. (2018). Additive Phenotypes Underlie Epistasis of Fitness Effects. *Genetics, 208*(1), 339-348. doi:10.1534/genetics.117.300451

Salverda, M. L. M., Koomen, J., Koopmanschap, B., Zwart, M. P., & de Visser, J. (2017). Adaptive benefits from small mutation supplies in an antibiotic resistance enzyme. *Proc Natl Acad Sci U S A, 114*(48), 12773-12778. doi:10.1073/pnas.1712999114

Santos-Lopez, A., Bernabe-Balas, C., Ares-Arroyo, M., Ortega-Huedo, R., Hoefer, A., San Millan, A., & Gonzalez-Zorn, B. (2017). A Naturally Occurring Single Nucleotide Polymorphism in a Multicopy Plasmid Produces a Reversible Increase in Antibiotic Resistance. *Antimicrob Agents Chemother, 61*(2). doi:10.1128/AAC.01735-16

Stalder, T., & Top, E. (2016). Plasmid transfer in biofilms: a perspective on limitations and opportunities. *NPJ Biofilms Microbiomes, 2*. doi:10.1038/npjbiofilms.2016.22

Steenackers, H. P., Parijs, I., Foster, K. R., & Vanderleyden, J. (2016). Experimental evolution in biofilm populations. *FEMS Microbiol Rev, 40*(3), 373-397. doi:10.1093/femsre/fuw002

Su, X. Z., Chen, J., Mizushima, T., Kuroda, T., & Tsuchiya, T. (2005). AbeM, an H+-coupled Acinetobacter baumannii multidrug efflux pump belonging to the MATE family of

976 transporters. *Antimicrob Agents Chemother, 49*(10), 4362-4364.
977 doi:10.1128/AAC.49.10.4362-4364.2005
978 Traverse, C. C., Mayo-Smith, L. M., Poltak, S. R., & Cooper, V. S. (2013). Tangled bank of
979 experimentally evolved Burkholderia biofilms reflects selection during chronic
980 infections. *Proc Natl Acad Sci U S A, 110*(3), E250-259. doi:10.1073/pnas.1207025110
981 Tseng, B. S., Zhang, W., Harrison, J. J., Quach, T. P., Song, J. L., Penterman, J., . . . Parsek, M.
982 R. (2013). The extracellular matrix protects Pseudomonas aeruginosa biofilms by
983 limiting the penetration of tobramycin. *Environ Microbiol, 15*(10), 2865-2878.
984 doi:10.1111/1462-2920.12155
985 Turner, C. B., Marshall, C. W., & Cooper, V. S. (2018). Parallel genetic adaptation across
986 environments differing in mode of growth or resource availability. *Evolution Letters,*
987 *2*(4), 355-367. doi:doi:10.1002/evl3.75
988 Van den Bergh, B., Swings, T., Fauvart, M., & Michiels, J. (2018). Experimental Design,
989 Population Dynamics, and Diversity in Microbial Experimental Evolution.
990 *Microbiology and Molecular Biology Reviews, 82*(3), e00008-00018.
991 doi:10.1128/mmbr.00008-18
992 Ventola, C. L. (2015). The antibiotic resistance crisis: part 1: causes and threats. *P T, 40*(4),
993 277-283.
994 Vogwill, T., & MacLean, R. C. (2015). The genetic basis of the fitness costs of antimicrobial
995 resistance: a meta-analysis approach. *Evol Appl, 8*(3), 284-295. doi:10.1111/eva.12202
996 Walters, M. C., 3rd, Roe, F., Bugnicourt, A., Franklin, M. J., & Stewart, P. S. (2003).
997 Contributions of antibiotic penetration, oxygen limitation, and low metabolic activity to
998 tolerance of Pseudomonas aeruginosa biofilms to ciprofloxacin and tobramycin.
999 *Antimicrob Agents Chemother, 47*(1), 317-323.
1000 Wang, Y.-C., Huang, T.-W., Yang, Y.-S., Kuo, S.-C., Chen, C.-T., Liu, C.-P., . . . Lee, Y.-T.
1001 (2018). Biofilm formation is not associated with worse outcome in Acinetobacter
1002 baumannii bacteraemic pneumonia. *Scientific Reports, 8*(1), 7289. doi:10.1038/s41598-
1003 018-25661-9
1004 Warner, D. M., Folster, J. P., Shafer, W. M., & Jerse, A. E. (2007). Regulation of the MtrC-
1005 MtrD-MtrE efflux-pump system modulates the in vivo fitness of Neisseria gonorrhoeae.
1006 *J Infect Dis, 196*(12), 1804-1812. doi:10.1086/522964
1007 Warner, W. A., Kuang, S. N., Hernandez, R., Chong, M. C., Ewing, P. J., Fleischer, J., . . . Xu,
1008 H. H. (2016). Molecular characterization and antimicrobial susceptibility of
1009 Acinetobacter baumannii isolates obtained from two hospital outbreaks in Los Angeles
1010 County, California, USA. *BMC Infect Dis, 16*, 194. doi:10.1186/s12879-016-1526-y
1011 Wickham, H. (2007). Reshaping Data with the reshape Package. *Journal of Statistical Software,*
1012 *21(12)*, 1-20.
1013 Wickham, H. (2016). *Elegant Graphics for Data Analysis*. New York: Springer-Verlag.
1014 Wickham, H., François, R., Henry, L., & Müller, K. (2018). dplyr: A Grammar of Data
1015 Manipulation. R package version 0.7.8. https://CRAN.R-project.org/package=dplyr.
1016 Wistrand-Yuen, E., Knopp, M., Hjort, K., Koskiniemi, S., Berg, O. G., & Andersson, D. I.
1017 (2018). Evolution of high-level resistance during low-level antibiotic exposure. *Nat*
1018 *Commun, 9*(1), 1599. doi:10.1038/s41467-018-04059-1
1019 Wolcott, R. D. (2017). Biofilms cause chronic infections. *J Wound Care, 26*(8), 423-425.
1020 doi:10.12968/jowc.2017.26.8.423
1021 Wolcott, R. D., Rhoads, D. D., Bennett, M. E., Wolcott, B. M., Gogokhia, L., Costerton, J. W.,
1022 & Dowd, S. E. (2010). Chronic wounds and the medical biofilm paradigm. *J Wound*
1023 *Care, 19*(2), 45-46, 48-50, 52-43. doi:10.12968/jowc.2010.19.2.46966
1024 Yang, H., Hu, L., Liu, Y., Ye, Y., & Li, J. (2016). Detection of the plasmid-mediated quinolone
1025 resistance determinants in clinical isolates of Acinetobacter baumannii in China. *J*
1026 *Chemother, 28*(5), 443-445. doi:10.1179/1973947815y.0000000017
1027 Yen, P., & Papin, J. A. (2017). History of antibiotic adaptation influences microbial
1028 evolutionary dynamics during subsequent treatment. *PLoS Biol, 15*(8), e2001586.
1029 doi:10.1371/journal.pbio.2001586

1030 Yoon, E. J., Chabane, Y. N., Goussard, S., Snesrud, E., Courvalin, P., De, E., & Grillot-
1031 Courvalin, C. (2015). Contribution of resistance-nodulation-cell division efflux systems
1032 to antibiotic resistance and biofilm formation in Acinetobacter baumannii. *MBio, 6*(2).
1033 doi:10.1128/mBio.00309-15
1034 Zhao, X., & Drlica, K. (2002). Restricting the selection of antibiotic-resistant mutant bacteria:
1035 measurement and potential use of the mutant selection window. *J Infect Dis, 185*(4),
1036 561-565. doi:10.1086/338571

1037